Published in final edited form as:
Magn Reson Imaging. 2009 June ; 27(5): 594–600. doi:10.1016/j.mri.2008.10.006.

Accounting for Nonspecific Enhancement in Neuronal Tract Tracing using Manganese Enhanced MRI

Kai-Hsiang Chuang* and **Alan P. Koretsky**
Laboratory of Functional and Molecular Imaging, National Institute of Neurological Disorders and Stroke, National Institutes of Health, Bethesda, MD 20892, USA

Abstract

Manganese enhanced MRI (MEMRI) is an emerging technique for tracing neuronal pathways *in vivo*. However, manganese may leak into blood vessels or cerebrospinal fluid (CSF) after local injection, and can be circulated to and taken up by brain regions that may not have connections to the targeted pathways. Comparing enhancement time-courses after intranasal injection with intravenous infusion of $MnCl_2$ in rats, the early enhancements in the pituitary gland (Pit) and hippocampus indicate the contrasts in those regions in the olfactory tract-tracing experiment were caused by such systemic effects. Since the Pit has easy access to manganese from the blood and its signal is proportional to other brain regions after intravenous infusion, it was used as an internal reference for the systemic effects. Applying intensity normalization by the Pit signal to tract-tracing data from the olfactory bulb led to reduced contrast in the hippocampus. These results demonstrate that nonspecific enhancements in MEMRI tract-tracing studies may have to be taken into account and that normalization by the Pit signal can compensate these effects.

Keywords

tract tracing; pituitary gland; olfactory pathways; molecular imaging; MRI

Introduction

Mapping cortical and subcortical neuronal connections is an important aspect of understanding brain function. Recent advances in manganese-enhanced MRI (MEMRI) provide a new approach for visualizing neuronal pathways *in vivo* [1]. By injecting Mn^{2+} into specific sites in the brain or peripheral regions, MEMRI tract tracing has been demonstrated in many systems and species, such as the olfactory pathway in rodents through intranasal injection [2,3] or intracerebral injection [4]; the visual pathway via intra-vitreous injection [2,5–7]; the somatosensory pathway [8,9] and basal ganglia pathway [10,11] by stereotaxic injection; and the song control pathway in birds [12]. Transport of Mn^{2+} across 2 to 3 synapses has been observed [2,4,6,7,10].

*Correspondence to: Kai-Hsiang Chuang, Ph.D., Building 10, Room 3D17, 10 Center Drive, MSC 1488, Bethesda, MD 20892, Telephone: (301) 594-7314, Fax: (301) 435-8228, chuangk@ninds.nih.gov.
*Current address: Laboratory of Molecular Imaging, Singapore Bioimaging Consortium, 11 Biopolis Way, Helios #02-02, Singapore 138667. Telephone: +65-64788764. chuang_kai_hsiang@sbic.a-star.edu.sg

Although enhancements in specific pathways can be observed, enhancement has also been found in regions outside the expected neuronal pathway. For example, in studies tracing the olfactory pathway, enhancement in the pituitary gland (Pit), which does not have direct connection with the olfactory bulb (OB), has been reported [2,3]. These results raise the issue of whether nonspecific enhancement contributes to MEMRI tract tracing. For instance, in intranasal injection, Mn^{2+} would get into blood vessels in the nostril epithelium and be circulated to the brain. Although Mn^{2+} does not cross the blood-brain barrier (BBB) readily, it can enter the brain through the choroid plexus-blood junction [13–15]. Similar problem would arise if one tries tracing from other peripheral areas to the brain. Even with stereotaxic intracerebral injection, if the injection site is close to ventricular space (e.g., amygdala or hippocampus), Mn^{2+} can also be circulated throughout the brain via the cerebrospinal fluid (CSF) [16,17]. Therefore, brain tissues can accumulate Mn^{2+} from the blood stream or CSF. Indeed, this is the approach taken by MEMRI neuroarchitecture studies where systemic administration of $MnCl_2$ enhances brain MRI in interesting ways [13,17]. Even though the amount of Mn^{2+} which gets into the blood or CSF from a focal injection site is small, it can cause significant enhancement in regions that tend to accumulate high levels of manganese, such as the Pit, cerebellum or hippocampus. This means not only regions outside a pathway (e.g., the Pit) but also regions that are potentially within a pathway (e.g., hippocampus) could be enhanced by these indirect routes.

In this study, we investigated the possible nonspecific enhancement in an MEMRI tract-tracing experiment and ways to reduce it. Mn^{2+} is transported at a rate of 1 – 6 mm/h in axons [2,5, 8,11] so that typically 24 to 72 h is needed for Mn^{2+} to be transported in sufficient quantities to target regions. By comparing signal time courses with intravenous (i.v.) administration of Mn^{2+}, nonspecific enhancement due to systemic effects could be discriminated. In addition, previous studies have shown that the Pit has rapid Mn^{2+} enhancement within an hour after systemic infusion and remains enhanced in rodents [13,14,18,19]. It was tested whether the Pit signal could be used as a reference for controlling nonspecific enhancement in MEMRI tract-tracing experiments.

Methods

Experiments were carried out in male Sprague-Dawley rats (150 – 255 g). All animal work followed the guidelines of the Animal Care and Use Committee of the National Institute of Neurological Disorders and Stroke, NIH (Bethesda, MD). To trace the neuronal connections in the olfactory pathway, 20 μL of 500 mM $MnCl_2$ (Sigma-Aldrich, St. Louis, MO) aqueous solution was injected into both nostrils of a rat ($N = 5$). No abnormal behavior was observed after injection. To evaluate the nonspecific enhancement in the brain, 5 rats received i.v. infusion of 9 mg/kg Mn^{2+}, which is close to the daily dietary dose of 10 mg/kg [20]. This dosage avoids saturating the tissue absorption capacity for manganese. Another 3 rats were infused with a higher dose (44 mg/kg) of Mn^{2+} to evaluate the dose dependence of tissue enhancement. This dose is about a quarter of the highest dose used in previous studies with i.v. infusion [13,14] and shall safely provide high tissue enhancement without saturating most of them. These rats were infused with 120 mM $MnCl_2$ at a rate of 2.25 mL/h by a syringe pump (Cole-Parmer Instrument, Vernon Hills, IL) under 1.0 – 2.0 % isoflurane anesthesia. During and after the infusion, their body temperatures were maintained by a warm water bath until fully awake. Then they were returned to cages for free access to food and water. No sign of abnormalities was observed.

MRI scans were conducted before, and at 1, 12, 24, 36 and 48 hours after Mn^{2+} administration. Rats were anesthetized with 1.5–2.5 % isoflurane in a 1:1:1 mixture of O_2:N_2:air using a nosecone and their heads were immobilized in a plastic stereotaxic holder. The rectal temperature was maintained at approximately 37°C using warm water circulation. Images were

acquired on an 11.7 T/31 cm horizontal magnet interfaced to a Bruker Avance console (Bruker BioSpin, Billerica, MA). A 70-mm diameter birdcage coil was used for homogeneous RF excitation and a 2 × 3 cm saddle-shaped surface coil was used for signal reception. The surface coil was carefully aligned with the eyes of the rats to minimize the position difference. T_1-weighted images were acquired by 3D rapid acquisition with relaxation enhancement (RARE) sequence with TR = 300 ms, effective TE = 10 ms and a RARE factor of 2. An axial slab with field-of-view of 38.4 × 25.6 × 25.6 mm^3 and matrix size of 192 × 128 × 128 was used to obtain 200-μm isotropic resolution.

Images acquired from the same animal at different times were manually registered to the image acquired before manganese injection. Region-of-interests (ROIs) were drawn on the major areas in the olfactory pathway according to the rat brain atlas [21] using AMIDE [22]. These regions included the OB, anterior olfactory nucleus (AON), piriform cortex (PCX), amygdala (AMG), and hippocampus (HC). The ROI for the OB was drawn in the anterior part of the bulb, which is close to where Mn^{2+} gets in the OB in the intranasal injection experiment. Other regions not in the olfactory pathway were also selected to evaluate nonspecific enhancements, such as the Pit, cortical gray matter (GM) in the somatosensory area and muscle in the neck. To average and compare data from different animals, regional signal-to-noise ratio (SNR) and two kinds of signal normalization were used. Regional SNR was calculated by dividing the mean signal in an ROI by the standard deviation in a noise region outside the head. Signal normalization was performed by dividing the mean signal in an ROI by the mean signal in the Pit or muscle. Statistical analysis was performed using Student's paired t-test; a value of $p < 0.05$ was considered significant.

Results

At 12 h after intranasal injection of Mn^{2+}, high contrast could be observed mainly in the OB and part of the AON, while enhancement could also be seen in more distant regions especially the HC and Pit (Fig. 1a, left column). At 24 h post-injection, major gray and white matter structures along the olfactory pathway, including the OB, AON, olfactory tubercle (Tu), PCX, and anterior commissure (AC) that connects bilateral PCX, were enhanced. In contrast, there were strong enhancements in the Pit, HC, and OB (Fig. 1a, right column) at 12 h after i.v. administration of 9 mg/kg (low dose) Mn^{2+}. The high enhancement in these areas compared to others suggested that they readily accumulated Mn^{2+}. At 24 h after infusion, contrast in most cortical and some subcortical gray matter areas were increased as well.

Fig. 1b and 1c show the progression of enhancement in the OB, HC, and Pit up to 48 h after intranasal injection ($N = 5$) and i.v. administration of 9 mg/kg of Mn^{2+} ($N = 5$), respectively. Although the HC and Pit doesn't have direct projections from the OB, both areas showed significant ($p < 0.05$, paired t-test) contrast as early as 12 h post-intranasal injection as compared to the 1 h post-injection time point. Significant enhancements were also detected in the HC and Pit at 12 h after i.v. infusion and the signals in the three areas kept increasing through out the 48 h period. The similar early enhancements in the Pit and HC under both intranasal and i.v. injections indicate that enhancements in these regions after intranasal injection were not due to axonal transport. In addition, the similar trends of signal increase in the Pit with other tissues (e.g., the HC) suggested that the Pit may be used as a reference for the systemic enhancement.

Fig. 2a shows the time courses normalized by the Pit signal after systemic infusion of 9 mg/kg of Mn^{2+}. The normalized signals at all the time points became insignificant compared to the first time point ($p > 0.1$, paired t-test). This demonstrates that intensity normalization by the Pit signal effectively reduced signal enhancements after systemic administration of $MnCl_2$. In contrast, intensity normalization using the muscle signal still showed similar

temporal variations in these brain regions (data not shown). This is probably due to the low level of muscle enhancement after systemic $MnCl_2$ infusion. Fig. 2b shows the SNR time courses of the Pit and PCX after i.v. infusion of 44 mg/kg (high dose; $N = 3$; solid lines) and 9 mg/kg (dashed lines) of $MnCl_2$. The Pit signal at the high dose condition maintained at a plateau after 1 h post-infusion while the PCX signal increased with a similar trend as in the low dose condition. Therefore, the capacity of Mn^{2+} uptake in the Pit may be saturated and thus could not serve as a reference for systemic effects at this high dose.

After normalizing the image intensity of the tract-tracing data by the Pit signal, the enhancements in the OB, AON, PCX, Tu and AC were still readily detectable but not in the HC or AMG (Fig. 3a). From the normalized time courses, the signals in the HC, AMG, and GM did not increase with time (Fig. 3b). The increasing signal in the PCX while decreasing in the OB indicates that Mn^{2+} continued to accumulate in the PCX after beginning to leave the OB at about 12 h after intranasal injection.

Discussion

We have demonstrated that some signal enhancement in a MEMRI tract-tracing experiment could come from systemically circulated Mn^{2+} and intensity normalization by the Pit signal could reduce this confound. Intranasal injection of substances is well known to be an effective route to administer drugs to the blood. Therefore, injection of $MnCl_2$ into the nostrils is particularly susceptible to nonspecific enhancements in MEMRI tract tracing. Stereotaxic injection directly into the brain may not cause as large systemic effects. However, injection sites close to ventricular space and tract tracing from peripheral sites to the brain may still be confounded by these effects.

Previous MEMRI studies have used SNR [5], intensity normalization to a tissue inside [23] or outside the brain, such as the muscle [11], that is not significantly enhanced to compare signal changes in different brain areas. However, these methods do not account for the possibility of systemic effects from Mn^{2+} that can leak into blood or CSF. Following the time course of signal enhancement enables distinguishing tracing from systemic effects because regions that readily accumulate Mn^{2+} from blood or CSF are predicted to show enhancements earlier than that due to axonal transport. However, this requires a large amount of MRI time. Applying the Pit normalization to the olfactory tract tracing data showed that nonspecific enhancements detected in the HC, AMG and GM were eliminated. Although the AMG does have direct projections from the OB, to detect this connection requires averaging multiple animals [3], or using a more sensitive quantitative T_1 imaging approach [4]. The HC tends to accumulate a lot of Mn^{2+} due to the nearby subventricular zone [14] as well as its high activity and the specific cell types that have large amounts of mitochondria and manganese superoxide dismutase [24]. Though the HC have indirect projection from the OB through the entorhinal cortex, it is less possible to be detected by the current protocol.

The reasons of using the Pit as an internal reference for systemic effects are anatomically easily delineated and, more importantly, its easy access to Mn^{2+} in the blood. Mn^{2+} is readily taken up by the Pit due both to high transport of Mn^{2+} [25,26] and a lack of the BBB. These make the Pit absorb Mn^{2+} earlier than other regions of the brain. Other circumventricular organs, such as pineal gland, median eminence, and the subfornical organ, also lack a BBB and would be good references for the systemic effects. Since the Pit is easier to identify and maintains similar trend of enhancement in the 48 h period studied, it is a good candidate area to control for systemic effects.

There are some drawbacks to the use of the Pit normalization approach. If there are significant amounts of Mn^{2+} being transported by neuronal tracts to the Pit, the normalization could render

these tracts undetectable and reduce the sensitivity in other tracts. Furthermore, using this approach assumes consistent Mn^{2+} uptake (and release) rates during the observation period. The accumulation of Mn^{2+} in the Pit may be dependent on the Pit activity which is controlled by a variety of hormones. For example, thyrotropin-releasing hormone, which is involved in the regulation of body temperature, can increase the influx of Ca^{2+} and Mn^{2+} to anterior pituitary cells [27]. If there are some stimuli or environmental changes that could alter the activity in the Pit during the experimental period, other circumventricular organs may be a better reference for intensity normalization.

Another issue is that accumulation of Mn^{2+} in the Pit is time and dose dependent. As shown in Fig.2b, the Pit signal (blue dashed line) increased gradually at the first 12 h after i.v. infusion and then maintained at a certain level. It should be noted that the increasing Pit signal may cause underestimation of the Mn^{2+} transport rate in axons if the intensity is normalized by the Pit signal during this period. Besides, the Pit may be saturated at high dose of Mn^{2+}. This will make the Pit signal act differently from other brain tissues and no longer be suitable to serve as a reference for intensity normalization. For example, i.v. infusion of 44 mg/kg of Mn^{2+} caused the enhancement in the Pit to reach a plateau 1 h after the infusion while signals in other brain tissues were still rising (Fig. 2b). Local injection of Mn^{2+} for tract tracing is not expected to lead to high levels of blood Mn^{2+}. The intranasal injection with 500 mM of Mn^{2+} did not saturate the Pit signal, but care must be taken if higher doses are used. In addition to saturating the transport, another reason that MRI signal can saturate is that high concentrations of Mn^{2+} can cause T_2 shortening, which results in a reduction of signal intensity to offset increases from the T_1-weighted imaging sequence used. Using quantitative T_1 mapping can avoid this T_2 effect.

It should also be noted that although the entire Pit is enhanced after systemic administration, enhancement in the Pit is not homogeneous. It was observed that the intermediate Pit is preferentially enhanced by Mn^{2+} [28]. Besides, the anterior Pit has higher signal increase than the posterior Pit [24]. Since the intermediate Pit is very thin, it was not easily distinguished at the resolution used in the current study. We used an ROI to average signal from most of the anterior Pit. Although including the other parts of the Pit would not make the normalization invalid, the sensitive to the systemic effects would be different.

Since tissue T_1 is generally longer at higher magnetic field and the relaxivity of Mn^{2+} didn't change much at high field [15,29,30], the T_1 shortening and the resulted signal change due to Mn^{2+} will be smaller at a lower field (e.g., 4.7T) than at a higher field (e.g., 11.7T used in this study). Nonspecific enhancement at lower field will also be smaller but would not differ much with that at higher field due to small amount of Mn^{2+} distributed nonspecifically in a tract tracing study. Therefore, nonspecific enhancement could still be an issue at lower magnetic field.

The intensity uniformity in the brain due to B_1 field inhomogeneity and positioning of RF coils is another factor that can affect the result of signal normalization especially when surface coils are used for detection. In this study, we used a volume transmit coil to provide homogeneous excitation and a saddle-shaped receive coil to achieve good penetration depth in the ventral part of the brain. However, there was still about a 20% signal variation across the whole brain. By careful positioning of the receive coil, this variation could be kept consistent from animal to animal and minimized effects on the normalization. It is possible to use a variety of techniques to account for signal intensity variations such as correcting coil sensitivity profiles [31] or T_1 mapping [4].

In conclusion, signal enhancement of the brain caused by Mn^{2+} entering the blood or CSF can lead to nonspecific enhancements in MEMRI tract-tracing experiments. The Pit is a useful

indicator to assess the extent of systemic effects. Furthermore, any systemic effects that do occur in the brain can be effectively reduced by normalizing the image intensity with respect to the Pit signal. This normalization procedure enabled well defined pathways and signal time courses to be obtained.

Acknowledgements

We would like to thank Ms Torri Wilson for assisting the animal preparation and Dr. Hellmut Merkle for building the RF coils. This research was supported by the Intramural Research Program of the NINDS, NIH.

References

1. Pautler RG. In vivo, trans-synaptic tract-tracing utilizing manganese-enhanced magnetic resonance imaging (MEMRI). NMR Biomed 2004;17(8):595–601. [PubMed: 15761948]
2. Pautler RG, Silva AC, Koretsky AP. In vivo neuronal tract tracing using manganese-enhanced magnetic resonance imaging. Magn Reson Med 1998;40(5):740–748. [PubMed: 9797158]
3. Cross DJ, Minoshima S, Anzai Y, Flexman JA, Keogh BP, Kim Y, Maravilla KR. Statistical mapping of functional olfactory connections of the rat brain in vivo. Neuroimage 2004;23(4):1326–1335. [PubMed: 15589097]
4. Chuang KH, Koretsky A. Improved neuronal tract tracing using manganese enhanced magnetic resonance imaging with fast T(1) mapping. Magn Reson Med 2006;55(3):604–611. [PubMed: 16470592]
5. Watanabe T, Michaelis T, Frahm J. Mapping of retinal projections in the living rat using high-resolution 3D gradient-echo MRI with Mn2+-induced contrast. Magn Reson Med 2001;46(3):424–429. [PubMed: 11550231]
6. Thuen M, Singstad TE, Pedersen TB, Haraldseth O, Berry M, Sandvig A, Brekken C. Manganese-enhanced MRI of the optic visual pathway and optic nerve injury in adult rats. J Magn Reson Imaging 2005;22(4):492–500. [PubMed: 16161073]
7. Murayama Y, Weber B, Saleem KS, Augath M, Logothetis NK. Tracing neural circuits in vivo with Mn-enhanced MRI. Magn Reson Imaging 2006;24(4):349–358. [PubMed: 16677940]
8. Leergaard TB, Bjaalie JG, Devor A, Wald LL, Dale AM. In vivo tracing of major rat brain pathways using manganese-enhanced magnetic resonance imaging and three-dimensional digital atlasing. Neuroimage 2003;20(3):1591–1600. [PubMed: 14642470]
9. Allegrini PR, Wiessner C. Three-dimensional MRI of cerebral projections in rat brain in vivo after intracortical injection of MnCl2. NMR Biomed 2003;16(5):252–256. [PubMed: 14648884]
10. Pautler RG, Mongeau R, Jacobs RE. In vivo trans-synaptic tract tracing from the murine striatum and amygdala utilizing manganese enhanced MRI (MEMRI). Magn Reson Med 2003;50(1):33–39. [PubMed: 12815676]
11. Saleem KS, Pauls JM, Augath M, Trinath T, Prause BA, Hashikawa T, Logothetis NK. Magnetic resonance imaging of neuronal connections in the macaque monkey. Neuron 2002;34(5):685–700. [PubMed: 12062017]
12. Van der Linden A, Verhoye M, Van Meir V, Tindemans I, Eens M, Absil P, Balthazart J. In vivo manganese-enhanced magnetic resonance imaging reveals connections and functional properties of the songbird vocal control system. Neuroscience 2002;112(2):467–474. [PubMed: 12044464]
13. Aoki I, Wu YJ, Silva AC, Lynch RM, Koretsky AP. In vivo detection of neuroarchitecture in the rodent brain using manganese-enhanced MRI. Neuroimage 2004;22(3):1046–1059. [PubMed: 15219577]
14. Lee JH, Silva AC, Merkle H, Koretsky AP. Manganese-enhanced magnetic resonance imaging of mouse brain after systemic administration of MnCl2: dosedependent and temporal evolution of T1 contrast. Magn Reson Med 2005;53(3):640–648. [PubMed: 15723400]
15. Bock NA, Paiva FF, Nascimento GC, Newman JD, Silva AC. Cerebrospinal fluid to brain transport of manganese in a non-human primate revealed by MRI. Brain Res 2008;1198:160–170. [PubMed: 18243167]

16. Stieltjes B, Klussmann S, Bock M, Umathum R, Mangalathu J, Letellier E, Rittgen W, Edler L, Krammer PH, Kauczor HU, Martin-Villalba A, Essig M. Manganese-enhanced magnetic resonance imaging for in vivo assessment of damage and functional improvement following spinal cord injury in mice. Magn Reson Med 2006;55(5):1124–1131. [PubMed: 16602070]
17. Liu CH, D'Arceuil HE, de Crespigny AJ. Direct CSF injection of MnCl2 for dynamic manganese-enhanced MRI. Magn Reson Med 2004;51(5):978–987. [PubMed: 15122680]
18. London RE, Toney G, Gabel SA, Funk A. Magnetic resonance imaging studies of the brains of anesthetized rats treated with manganese chloride. Brain Res Bull 1989;23(3):229–235. [PubMed: 2819480]
19. Kuo YT, Herlihy AH, So PW, Bhakoo KK, Bell JD. In vivo measurements of T1 relaxation times in mouse brain associated with different modes of systemic administration of manganese chloride. J Magn Reson Imaging 2005;21(4):334–339. [PubMed: 15779025]
20. Subcommittee on Laboratory Animal Nutrition CoAN, Board on Agriculture, National Research Council. Nutrient requirements of laboratory animals: National Academy Press; 1995.
21. Paxinos, G.; Watson, C. The Rat Brain in Stereotaxic Coordinates. Academic Press; 1998.
22. Loening A, Gambhir S. AMIDE: A Free Software Tool for Multimodality Medical Image Analysis. Mol Imaging 2003;2(3):131–137. [PubMed: 14649056]
23. Yu X, Wadghiri YZ, Sanes DH, Turnbull DH. In vivo auditory brain mapping in mice with Mn-enhanced MRI. Nat Neurosci 2005;8(7):961–968. [PubMed: 15924136]
24. Watanabe T, Natt O, Boretius S, Frahm J, Michaelis T. In vivo 3D MRI staining of mouse brain after subcutaneous application of MnCl2. Magn Reson Med 2002;48(5):852–859. [PubMed: 12418000]
25. Nilsson P, Laursen H, Hillered L, Hansen AJ. Calcium movements in traumatic brain injury: the role of glutamate receptor-operated ion channels. J Cereb Blood Flow Metab 1996;16(2):262. [PubMed: 8594058]
26. Villalobos C, Alonso-Torre SR, Nunez L, Garcia-Sancho J. Functional ATP receptors in rat anterior pituitary cells. Am J Physiol 1997;273(6 Pt 1):C1963–C1971. [PubMed: 9435502]
27. Cui ZJ, Dannies PS. Thyrotropin-releasing hormone-mediated Mn2+ entry in perifused rat anterior pituitary cells. Biochem J 1992;283(Pt 2):507–513. [PubMed: 1575695]
28. Aoki, I.; Wu, YJ.; Silva, AC.; Koretsky, AP. Cortical Layers Revealed by Manganese Enhanced Magnetic Resonance Imaging (MEMRI) in the Rat Brain after Systemic Administration. Intl Soc Magn Reson Med 10th Scientific Meeting; Honolulu: Hawaii; 2002. p. 715
29. Silva AC, Lee JH, Aoki I, Koretsky AP. Manganese-enhanced magnetic resonance imaging (MEMRI): methodological and practical considerations. NMR Biomed 2004;17(8):532–543. [PubMed: 15617052]
30. Chuang, KH.; Koretsky, AP.; Sotak, CH. Temporal Changes in the T1 and T2 Relaxation Rates (ΔR1 and ΔR2) in the Rat Brain are Consistent with the Tissue- Clearance Rates of Elemental Manganese. Intl Soc Magn Reson Med 16th Scientific Meeting; Toronto, Canada: 2008. p. 531
31. Lin FH, Chen YJ, Belliveau JW, Wald LL. A wavelet-based approximation of surface coil sensitivity profiles for correction of image intensity inhomogeneity and parallel imaging reconstruction. Hum Brain Mapp 2003;19(2):96–111. [PubMed: 12768534]

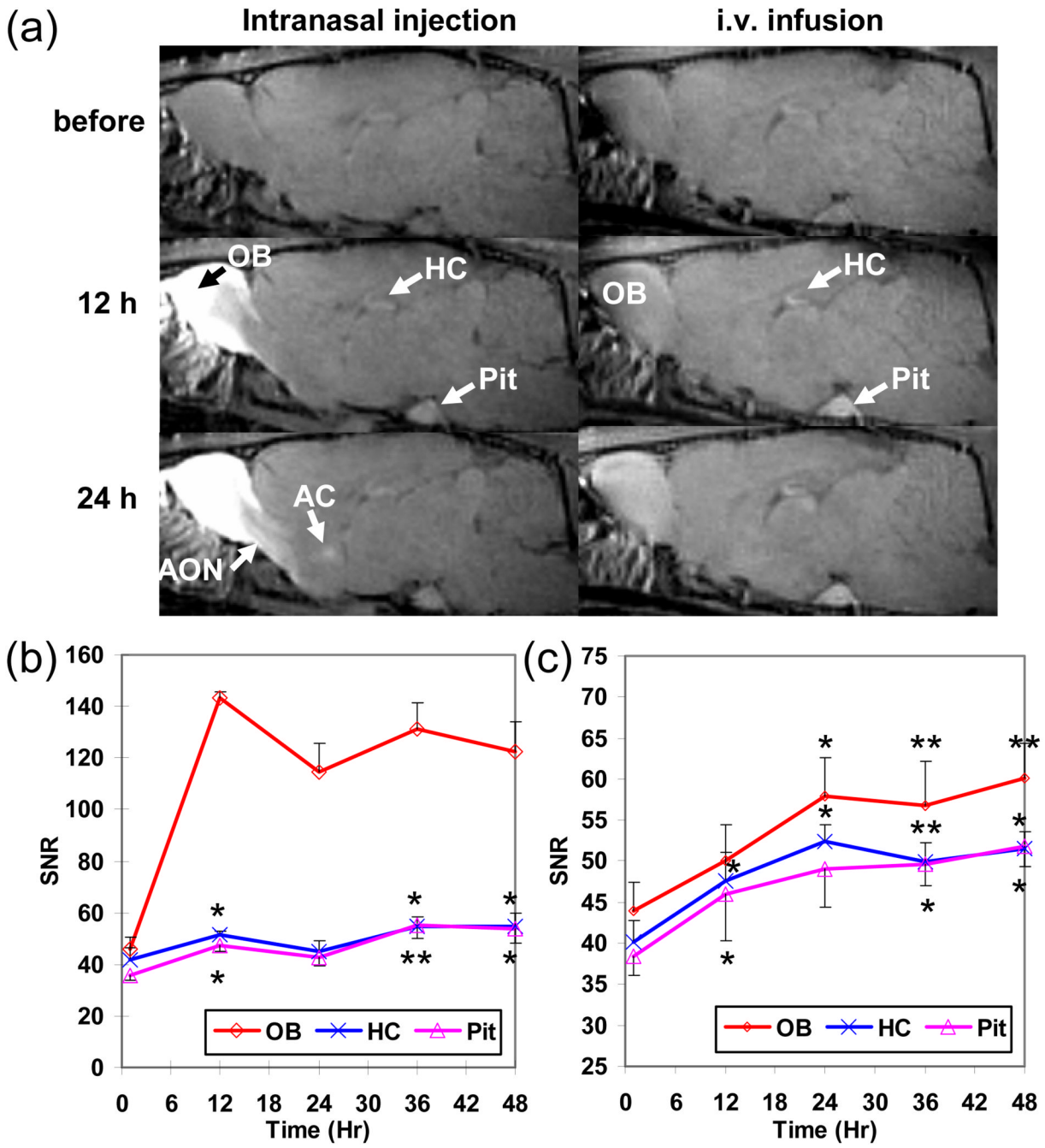

Fig 1.

(a) Time series T_1-weighted images of rat brains before and at 12 and 24 h after intranasal $MnCl_2$ injection (left column) and i.v. infusion of 9mg/kg of $MnCl_2$ (right column). The averaged SNR time courses of the OB, HC, and Pit at 1, 12, 24, 36, and 48 h after (b) intranasal injection and (c) i.v. infusion of 9 mg/kg of $MnCl_2$ (the error bar represents the standard error among animals). Significant early enhancement in HC and Pit indicates that the contrasts are due to systemic effects rather than tract tracing. (*: $p < 0.05$; **: $p < 0.01$, paired t-test compared to the first time point.)

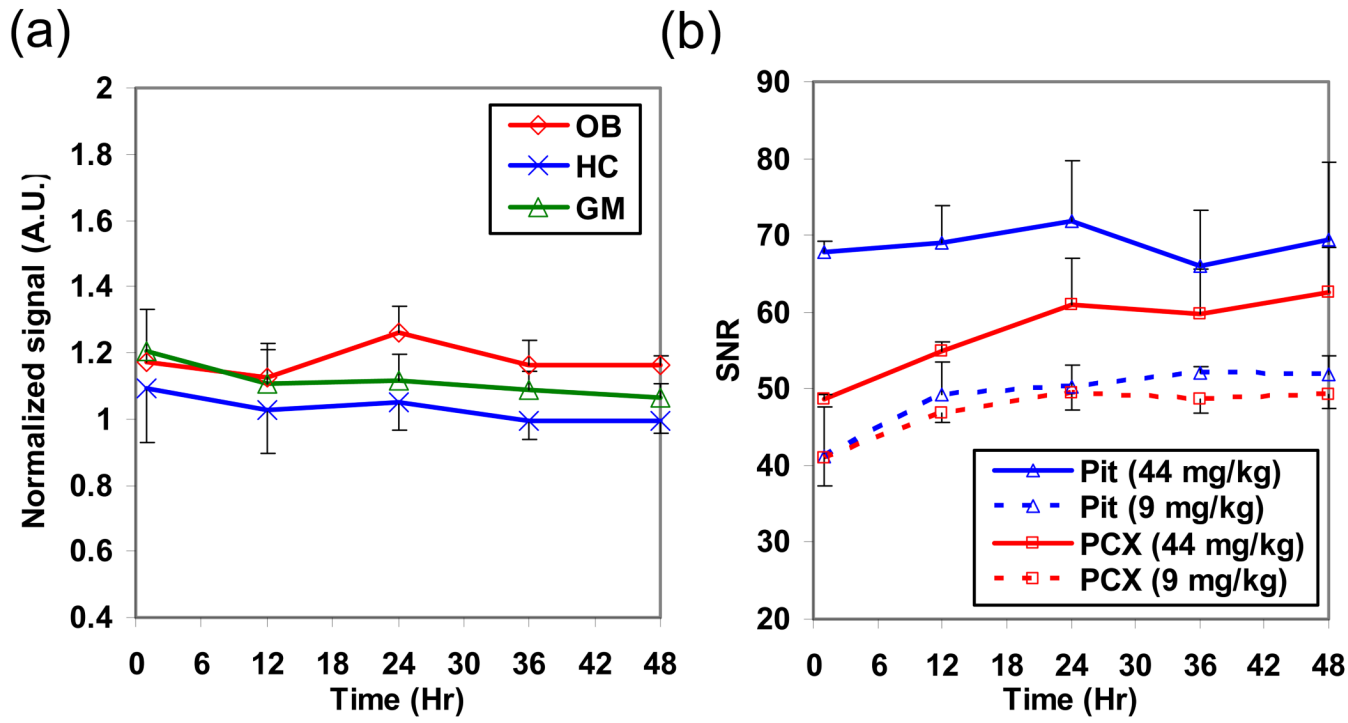

Fig. 2.

(a) The normalized signal time courses in the OB, HC, and GM by the Pit signal in rats with i.v. infusion of 9 mg/kg of $MnCl_2$ (N = 5; the error bar represents the standard error among animals). After the normalization, these tissues didn't have significant signal change at all the time points. (b) The SNR time courses in the Pit and PCX with i.v. infusion of 44 mg/kg (N = 3; solid lines) and 9 mg/kg (N = 5; dashed lines) of $MnCl_2$. At the high dose condition, the signal plateau in the Pit from 1h suggested that its capacity of absorbing Mn^{2+} may be saturated.

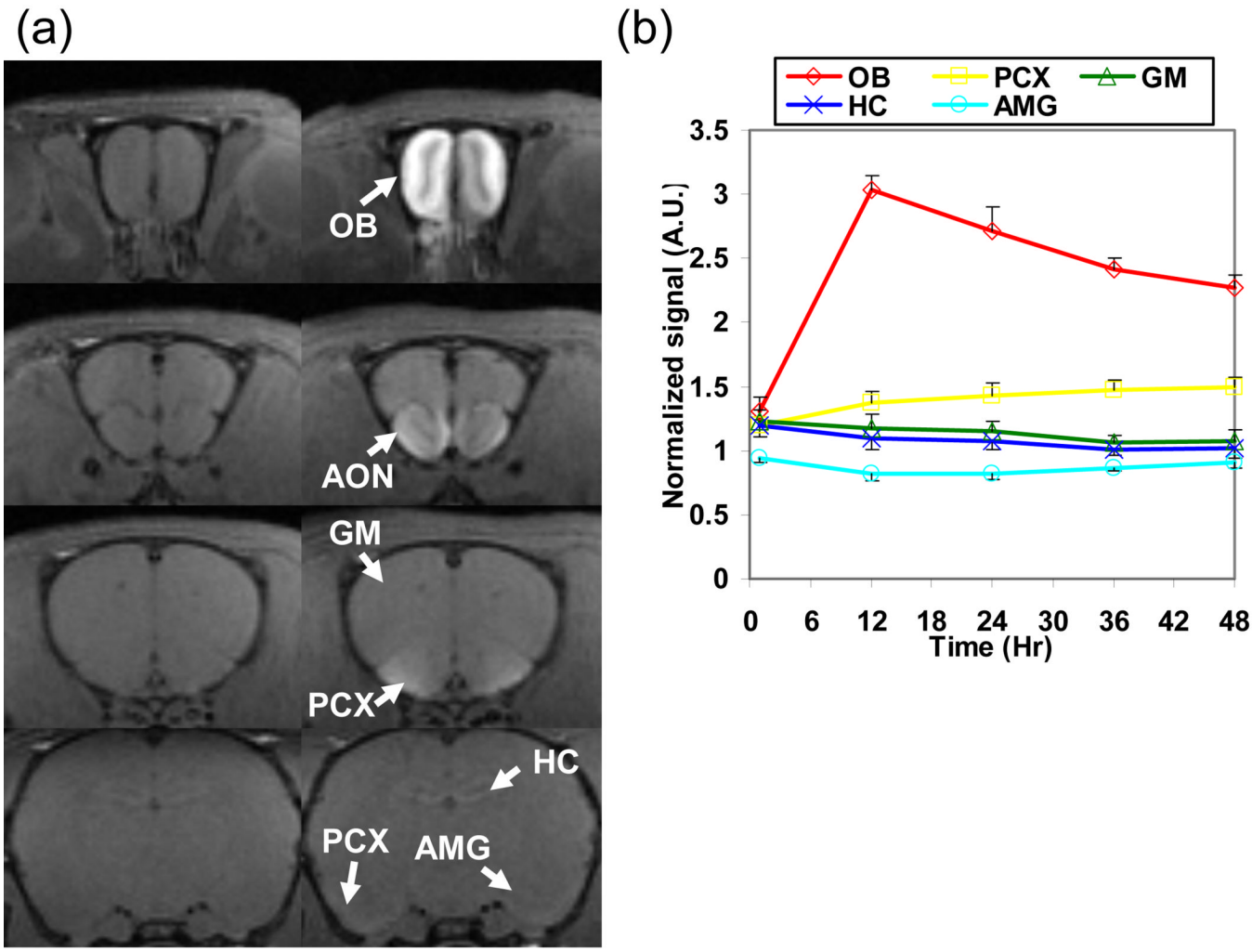

Fig 3.

(a) T_1-weighted images of a rat after intensity normalization by the Pit signal before (left column) and at 24 h (right column) after intranasal $MnCl_2$ injection. After normalization, significant contrast could still be seen in the OB, AON, PCX, and AC but not in the AMG and HC. (b) The averaged signal time courses (N = 5; the error bar represents the standard error among animals) of the OB, PCX, GM, HC, and AMG after normalized by the Pit signal show that only OB and PCX are enhanced.